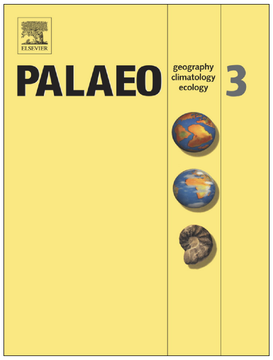

Shell sclerochronology and stable oxygen isotope ratios from the limpet Patella depressa Pennant, 1777: Implications for palaeoclimate reconstruction and archaeology in northern Spain

Asier García-Escárzaga, Igor Gutiérrez-Zugasti, Manuel R. González-Morales, Alvaro Arrizabalaga, Jana Zech, Patrick Roberts

PII: S0031-0182(20)30471-5

DOI: https://doi.org/10.1016/j.palaeo.2020.110023

Reference: PALAEO 110023

To appear in: *Palaeogeography, Palaeoclimatology, Palaeoecology*

Received date: 1 April 2020

Revised date: 9 September 2020

Accepted date: 10 September 2020

Please cite this article as: A. García-Escárzaga, I. Gutiérrez-Zugasti, M.R. González-Morales, et al., Shell sclerochronology and stable oxygen isotope ratios from the limpet Patella depressa Pennant, 1777: Implications for palaeoclimate reconstruction and archaeology in northern Spain, *Palaeogeography, Palaeoclimatology, Palaeoecology* (2020), https://doi.org/10.1016/j.palaeo.2020.110023

Shell sclerochronology and stable oxygen isotope ratios from the limpet *Patella depressa* Pennant, 1777: Implications for palaeoclimate reconstruction and archaeology in northern Spain

Asier García-Escárzaga[1,2,*] a.garcia.escarzaga@gmail.com, Igor Gutiérrez-Zugasti[3] fernandoigor.gutierrez@unican.es, Manuel R. González-Morales[3] manuelramon.gonzalez@unican.es, Alvaro Arrizabalaga[2] alvaro.arrizabalaga@ehu.eus, Jana Zech[1] zech@shh.mpg.de, Patrick Roberts[1,4] roberts@shh.mpg.de

[1]Department of Archaeology, Max Planck Institute for the Science of Human History. Kahlaische Strasse 10. D-07745 Jena, Germany.

[2]Department of Geography, Prehistory and Archaeology, University of the Basque Country (UPV/EHU), C/ Tomás y Valiente s/n, 01006, Vitoria-Gasteiz, Spain.

[3]Instituto Internacional de Investigaciones Prehistóricas de Cantabria (Universidad de Cantabria, Gobierno de Cantabria, Grupo Santander), Edificio Interfacultativo de la Universidad de Cantabria, Avda. Los Castros s/n. 39005. Santander, Spain.

[4]School of Social Sciences, University of Queensland, St Lucia, Queensland 4072, Australia.

[*]Corresponding author:

Abstract

Stable oxygen isotope ratios of mollusc shells ($\delta^{18}O_{shell}$) offer the possibility to reconstruct coastal resource exploitation patterns and changes in the oceanographic conditions of direct relevance to past human populations. This method relies on the fact that shell carbonate is deposited by molluscs in equilibrium with their surrounding environment and actualistic investigation of modern specimens is needed to ensure that selected species can be used as accurate palaeoclimate indicators. The limpet *Patella depressa* Pennant, 1777 is one of the most common mollusc species found in Holocene archaeological assemblages along the Atlantic coast of Europe. However, this taxon has not, to date, been tested as a seawater palaeothermometer. Here, we explore the ability of *P. depressa* to be used as an environmental recorder in this littoral region, specifically in northern Iberia where we obtained live-collected specimens throughout the year. We undertook sclerochronological investigations combining observations of incremental shell growth patterns with $\delta^{18}O_{shell}$ values. Carbonate samples were taken on (i) the ventral margins of shells collected alive year-round in order to test for isotopic equilibrium and (ii) along the axis of maximum shell growth of four modern specimens to decipher the shell growth pattern of this species. Isotopic data showed that calcium carbonate is precipitated in predictable isotopic disequilibrium with the ambient seawater ($R^2 = 0.95$; $p < 0.0001$), reporting a consistent offset of +1.08‰. Some periods of growth cessation were observed in the shells when thermal tolerances were exceeded in winter and occasionally in summer. Nevertheless, estimated seawater temperatures from modern shell $\delta^{18}O_{shell}$ values agreed closely with instrumentally measured temperatures ($R^2 = 0.88–0.93$; $p < 0.0001$) and correctly reflected seasonal temperature patterns. As a result, multi-proxy analysis of *P. depressa* shells can provide a high-resolution palaeothermometer with significant implications for future palaeoclimate and archaeological studies along the Atlantic coast of Europe.

Keywords: Sea Surface Temperature, Mollusc Shells, Palaeothermometer, Environmental Archive, Marine Resources, Atlantic Europe.

1. Introduction

Palaeoclimate studies are increasingly focusing on methodologies that enable high-resolution insights into seasonality, especially given the importance of annual fluctuations in temperature and precipitation for human subsistence and economic organisation (Arzell and Hoelzmann, 2000; Baldini et al., 2008; Fabre et al., 2011; Pederzani and Britton, 2019). A number of investigations have already extensively demonstrated that stable oxygen isotope ratios derived from archaeologically-recovered marine mollusc shells ($\delta^{18}O_{shell}$) can act as powerful recorders of the seasonal seawater temperature variations experienced year-round by a sample in the past (e.g., Andrus, 2011; Bailey et al., 1983; Leng and Lewis, 2016; Owen et al., 2002). This proxy primarily relies on the fact that the geochemical signatures of a mollusc species reflect the immediate marine environmental conditions, i.e., oxygen isotope composition of the seawater and seawater temperatures, during the calcium carbonate calcification process (Epstein et al., 1953; Grossman and Ku, 1986). Given the significance of marine resources to human forager diets, from some of the earliest *Homo sapiens* populations in southern and northern Africa to Mesolithic communities producing dense shell middens in the Holocene, this methodology offers a way to reconstruct the impact of intra-annual environmental changes on marine environments exploited by past societies (Ferguson et al., 2011; Hallmann et al., 2013; Schöne et al., 2004; Wanamaker et al., 2011; Wang et al., 2012).

In these contexts, $\delta^{18}O_{shell}$ values have been used to not only determine changing patterns of seawater temperature in the past but also the season of harvest of particular mollusc species (Branscombe et al., 2020; Burchell et al., 2018; Colonese et al., 2012; Hausman and Meredith-Williams, 2017; Prendergast et al., 2016). Evaluating the season(s) when molluscs were collected by hominin populations is crucial to better understand littoral resource exploitation patterns of past populations, especially if shellfish had an important role in their subsistence strategies, as well as seasonal foraging practices and mobility of a given population more broadly. One prominent case is the Atlantic coast of Europe during the Early and Middle Holocene (García-Escárzaga and Gutiérrez-Zugasti, in press). The European Mesolithic (ca. 11–6 cal kyr B.P.) along the Atlantic littoral is generally characterised by an increase in the consumption of coastal resources (Fontanals-Coll et al., 2014; Guiry et al., 2015; Schulting and Richards, 2001), including a variety of different shellfish species, resulting in the formation of massive shell middens in coastal areas that can cover an area of up to 6000 m^2 and have been argued to have sustained increasingly sedentary populations during this period (Gutiérrez-Zugasti et al., 2011; Milner et al., 2007).

Stable oxygen isotope analysis of mollusc shells offers the opportunity to greatly improve our understandings of marine foraging patterns at archaeological sites (Deith and Sackleton, 1986; García-Escárzaga et al., 2019a; Mannino et al., 2003). However, before deciphering paleoclimate conditions or reconstructing seasonal exploitation patterns from ancient shell remains of a given species, the proxy must first be calibrated using modern (live-caught) representatives (Schöne, 2008). To test if calcium carbonate calcification does indeed occur in equilibrium with the surrounding environment, shell oxygen isotopes ($\delta^{18}O_{shell}$) must be compared with both the stable oxygen isotope measurements of seawater ($\delta^{18}O_{sw}$) and seawater temperatures (ST) (Colonese et al., 2009; Mannino et al., 2008; Hallmann et al., 2009). Ideally, modern samples should come from the same region where the archaeological shells are recovered. These actualistic investigations have been developed in many parts of the world, including the Atlantic coast of Europe (Carré et al., 2005; Colonese et al., 2017; Prendergast et al., 2013; Schöne et al., 2003, 2007; Wanamaker et al., 2007). Previous analyses conducted in western Europe have focused on topshells *Phorcus lineatus* (da Costa, 1778) (García-Escárzaga et al., 2019b; Gutiérrez-Zugasti et al., 2015; Mannino et al., 2003), limpets *Patella vulgata* Linnaeus, 1758 (Fenger et al., 2007; Gutiérrez-Zugasti et al., 2017; Surge et al., 2013) and bivalves *Mytilus galloprovincialis* Lamarck, 1819 (Milano et al., 2020) as effective seawater palaeothermometers. However, the limpet *Patella depressa* Pennant, 1777, has received almost no attention, despite being one of the most represented mollusc species in Holocene archaeological assemblages. For example, results recently obtained from the shell midden sites of El Mazo and El Toral III (northern Spain) have shown that *P. depressa* was the most exploited mollusc species at these sites after 8 cal kyr B.P., representing more than 25% of the total minimum number of molluscs recovered from these stratigraphic units (Bello-Alonso et al., 2015; García-Escárzaga, 2020).

In this study, we explore the potential of *P. depressa* as a climate recorder by conducting the first stable isotopic and sclerochronological calibration for this taxon. Modern samples from northern Iberia were harvested during different collection events covering one complete year. We investigated the stable oxygen isotope profiles and microgrowth lines/increments of these specimens to determine whether $\delta^{18}O_{shell}$ values of shell carbonate for this species precipitated in isotopic equilibrium with the surrounding environment. More specifically, we investigated whether seasonal growth patterns of *P. depressa* in northern Iberia tracked intra-annual seawater temperature variations. Our results provide insights into the possible causes of some observed growth cessations (where relevant) and the accuracy of seawater temperature reconstruction using $\delta^{18}O_{shell}$ values of *P. depressa*. We argue that the data presented has significant, positive implications for future paleoclimate and archaeological studies along the Atlantic coast of Europe given the documented abundance of this species in archaeological assemblages at a number of Mesolithic sites.

2. Background

2.1 Study area: geographical, environmental and marine conditions

The coastal area of northern Iberia, in the Cantabrian region (Fig. 1a), is defined by oceanic, humid, and temperate climatic conditions, exhibiting four well-differentiated seasons. According to the Köppen climate classification, these conditions can be defined as mesothermal and, more precisely, as a Cfp type (temperate, without a dry season and with warm summer). The mean annual atmospheric temperature (15–16ºC) is higher than expected for this latitude (ca. 43ºN) as a consequence of the influence of the North Atlantic Current. The coldest month is January with an average temperature of 9–10ºC and the warmest month is August with an average temperature of 20–22ºC. Mean annual rainfall between 1981–2010 was 1100 mm in Santander. From October to April, the area receives more than 100 mm of precipitation per month (with 160 mm, November is the wettest month). Rainfall decreases considerably during the warmer months of May to September (with 50 mm, July is the driest month) (Source: National Meteorology Agency, http://www.aemet.es). The higher rainfall in comparison with more southerly regions on the Iberian Peninsula plateau is a result of the Foehn Effect as the mountains prevent the clouds crossing inland to the plateau, a well-defined effect in areas located on the lee side of a mountain range (Usabiaga et al., 2004). The Cantabrian Sea (southern Bay of Biscay) represents a boundary between subtropical and boreal conditions in the Eastern Atlantic. In terms of marine conditions, the study area is characterised by semidiurnal tides and by fortnightly neap and spring tides. The minimum and maximum tidal amplitude during neap and spring tides are ca. 1 m and ca. 5 m, respectively (Source: http://www.puertos.es). The seawater temperature in the central part of the Cantabrian region (data for Santander) follows a seasonal warming and cooling pattern, ranging from ca. 23 to ca. 11 ºC. While the coldest temperatures are often reached in February or March depending on the year, the warmest temperatures typically occur from August to September (Source: Spanish Institute of Oceanography).

2.2 Biology and ecology of *Patella depressa* Pennant, 1777

The limpet *P. depressa* (Fig. 2a) is a marine gastropod that inhabits intertidal rocky shores from northern Africa to southwestern England and Wales (Fretter and Graham, 1976). According to its geographical distribution, this species is very well adapted to temperate water conditions (ca. 10-22 ºC), although it is able to survive to seawater temperatures near 0 ºC and daily air mean temperature of -2 ºC for the course of several months (Crisp, 1964). This species has recently increased its relative abundance in northern locations as a result of global warming (Hawkins et al., 2008), resulting in a replacement of the cold-adapted *P. vulgata* by this southern limpet species (Kendall et al., 2004). A previous study conducted on the Portuguese coast showed that *P. depressa* has a life span of no longer than three years (Guerra and Gaudencio, 1986). The length and morphology of this species varies depending on its position in the intertidal zone. Shells living on the upper shore are usually steeply-conical and very thick, whereas at lower levels they are polygonal, flattened, and thin. The limpets of this species can reach 45 mm in length (Orton and Southward, 1961). From a feeding point of view, *P. depressa* is considered a microphagous herbivore that feeds on both microscopic plants and macroalgae by grazing the rocky substrate using a horny tongue (radula) (Moore et al., 2007). Their spawning and gonadal development stages also vary depending on the latitude (Orton and Southward, 1961; Ribeiro et al., 2009). In northern Iberia, mature gonads are found all year-round except for during the summer months, while at least two main spawning events occur in January/February and April/June (Fernández et al., 2016).

3. Materials and methods

3.1 Modern shell collection programme

A total of 59 live-collected shell samples were obtained from 11 collection events carried out at Langre Beach (Cantabria, northern Spain, Fig. 1) (43º 28' 37'' N, 3º 41' 44'' W) between the 12th October 2011 and the 1st October 2012 (see Supplementary Material Table 1 for full list of collection dates). The specimens were gathered from the intertidal rocky shore and they were sacrificed immediately after collection by immersion in boiling water for one minute, thus avoiding further deposition of calcium carbonate. Following previous studies conducted on mollusc remains, the shells were treated with 30 vol% H_2O_2 for 48 h in order to remove any organic matter (Colonese et al., 2009; García-Escárzaga et al., 2019a, 2019b; Gutiérrez-Zugasti et al., 2017). A small experimental programme conducted on *P. depressa* shows that pretreatment using H_2O_2 does not have any effect on stable oxygen isotope values (Supplementary Material Table 2). Following cleaning of the collected shells, they were air-dried at ambient temperature. Finally, the size (length, width, and height) of each mollusc shell was measured using a digital calliper to the nearest 0.01 mm.

3.2 Monitoring environmental parameters

Data relating to the salinity and the stable oxygen isotope composition of seawater ($\delta^{18}O_{sw}$) were taken from previously published studies at Langre Beach covering the period between October 2011 and October 2012 (Gutiérrez-Zugasti et al., 2015, 2017). In these studies, a total of 20 seawater samples were collected throughout the year and measured for salinity and $\delta^{18}O_{sw}$. These investigations reported a mean salinity value of 35.6 PSU, ranging from 34.0 to 37.1 PSU. Meanwhile, published $\delta^{18}O_{sw}$ at Langre Beach exhibited maximum, minimum, and mean values of +0.55‰, +1.19‰, and +0.90‰, respectively, showing a range of +0.64‰. These results demonstrate the occurrence of fully marine conditions at Langre Beach, with only minor changes linked to annual hydrological balance, linked to higher freshwater runoff in spring and higher precipitation in October and November. This previous research also demonstrated that intra-annual variations of salinity in the region have a very low correlation with $\delta^{18}O_{sw}$ variations (Gutiérrez-Zugasti et al., 2017). Daily instrumental seawater temperature (T_{meas}) data was provided by the Spanish Institute of Oceanography (Santander, Cantabria) (Fig. 1), which is located close to Langre beach (< 10 km). The conditions of the sea are similar in both areas, with no influence of continental runoff or sea currents with different salinity levels. Information in relation to daily tide cycles and sea levels from 2010 to 2012 was obtained from the website of the Santander Port (Source: http://www.puertosantander.es) and the WXTide32 computer program (www.wxtide32.com).

3.3 Sampling procedures and stable oxygen isotope analysis

Following the methodological procedures utilized in previous investigations of limpet shells (Gutiérrez-Zugasti et al., 2017; Prendergast and Schöne, 2017), in this study, two sampling strategies were applied in order to obtain two different datasets. Firstly, one calcium carbonate sample was taken from the inner part of the shell aperture on five limpets gathered during each collection event, providing a total of 55 powder samples for stable oxygen isotope analysis. Carbonate samples were taken by milling along the perimeter of the innermost part of the shell edge with the aid of a manually-operated diamond drill (Fig. 2a). The stable oxygen isotope values ($\delta^{18}O_{shell}$) obtained from shell edges, which represent the last day/s of the mollusc life span, were compared with contemporaneous instrumentally-measured sea temperatures (T_{meas}) and with predicted $\delta^{18}O_{shell}$ values based on T_{meas} and $\delta^{18}O_{sw}$, in order to test for isotopic equilibrium.

Secondly, four limpets collected on 1st October 2012 (ID codes: LAN541, LAN545, LAN554 and LAN559) (Supplementary Material Table 1) were sampled sequentially along the axis of shell growth in order to obtain stable oxygen isotope profiles across their life spans. The selected specimens were partially coated with a metal epoxy resin along the axis of maximum growth (i.e., from the anterior to the posterior margin) to avoid the shell breaking when sectioned. Sectioning was performed using a Buehler Isomet low-speed saw and a diamond wheel (Fig. 2a). Two thick sections (~3 mm each) were obtained from each limpet, one for stable isotope analysis and the other for growth pattern analysis. The sections were fixed onto a glass microscope slide with metal epoxy resin and ground on glass plates using 600 and 800 SiC grit powder and polished with 1 μm diamond suspension grit until the internal growth lines and increments were clearly visible (Fig. 2b). A ‘growth increment' refers to that period when the mollusc is submerged and is precipitating carbonate (i.e. growing). Meanwhile, a 'growth line' forms between two increments when the mollusc is not submerged, and are usually related to the incorporation of organic material (i.e. not growing) (Schöne, 2008). In each case, one of the sections was used for sequential stable oxygen isotope analysis of carbonate, the other was used to analyse shell growth patterns. According to the methodology previously applied to several limpet species (Fenger et al., 2007; Ferguson et al., 2011; Gutiérrez-Zugasti et al., 2017), calcium carbonate samples were taken from the concentric cross-foliated calcite layer equivalent to the m + 2 layer (MacClintock, 1967) using a New Wave MicroMill and a 1 mm drill bit following the shell growth direction from the edge to the apex, and in parallel to visible growth increments (Fig. 2c). A total of 88, 96, 72 and 71 carbonate samples were taken on each of the specimens LAN541, LAN545, LAN554 and LAN559, respectively. The width of the sampling paths ranged between 80 and 250 µm, depending on the speed of growth of the shell at different points during its life span. This results in smaller distances close to the shell-edge where growth is lower and larger distances near the shell-apex where growth is faster.

All carbonate powder samples resulting from both sampling strategies mentioned above weighed more than 150 µg. They were then placed within borosilicate glass vials. Stable oxygen isotope analyses were performed in an IRMS Thermo Scientific DELTA V coupled to a Gas Bench II Interface at the Department of Archaeology, Max Planck Institute for Science of Human History (Jena, Germany). Each powder sample was dissolved in concentrated phosphoric acid at 70 ºC. Isotopic ratios were calibrated against international NBS-18 (–23.2‰) and NBS-19 standards (–2.20‰). The results obtained are reported as $\delta^{18}O$ (‰) relative to the Vienna Pee Dee Belemnite (V-PDB) standard. The mean analytical error of the instrument based on repeat measurement of an in-house MERCK carbonate standard was ±0.07‰.

3.4 Predicted $\delta^{18}O_{shell}$ and oxygen isotope-derived temperatures ($T_{\delta 18O}$)

In order to test for isotopic equilibrium, we compared $\delta^{18}O_{shell}$ values taken from the shell edge of the 55 individual samples collected through the year with predicted $\delta^{18}O_{shell}$ values calculated from T_{meas} and $\delta^{18}O_{sw}$ for each collection event. To test whether the temporal alignment of $\delta^{18}O_{shell}$ profiles from the four shells sampled sequentially was correctly performed, $\delta^{18}O_{shell}$ values were compared with predicted $\delta^{18}O_{shell}$ values calculated from daily T_{meas} and $\delta^{18}O_{sw}$ for Langre beach (Gutiérrez-Zugasti et al., 2015, 2017). To statistically determine whether calcium carbonate formed in equilibrium with the surrounding environment and, in the case of the four sequentially-samples shells, to verify if schlerochronological calendar alignments of $\delta^{18}O_{shell}$ values were accurate, the coefficient of determination (R^2) between measured $\delta^{18}O_{shell}$ and predicted $\delta^{18}O_{shell}$ values was calculated using a linear regression analysis in Microsoft Excel using the 'Data Analysis' application and regression option. To estimate daily $\delta^{18}O_{sw}$ values for those days without data, an interpolation between two known values was performed. Although this inevitably introduces some error, it enabled us to produce a $\delta^{18}O_{sw}$ value for each day. For the period prior to October 2011, no data on $\delta^{18}O_{sw}$ was available, so the average annual value of the period October 2011 – October 2012 (+0.90‰) (Gutiérrez-Zugasti et al., 2015, 2017) was used. Predicted $\delta^{18}O_{shell}$ values were calculated using the equilibrium fractionation equation for calcite and water proposed by Friedman and O'Neil (1977):

$$1000 \ln\alpha = 2.78 \times 10^{6} / T^{2} - 2.89 \qquad (1)$$

where T is the temperature measured in Kelvin and α is the fractionation between water and calcite described by the equation:

$$\alpha = (1000 + \delta^{18}O_{shell}\ (\text{V-SMOW ‰})) / (1000 + \delta^{18}O_{sw}\ (\text{V-SMOW ‰})) \qquad (2)$$

$\delta^{18}O_{shell}$ (V-PDB ‰) values were converted to the V-SMOW ‰ scale using the equation published by Coplen (1988):

$$\delta^{18}O\ \text{V-SMOW ‰} = 1.03091 \times \delta^{18}O\ \text{V-PDB ‰} + 30.91 \qquad (3)$$

Reconstructed seawater temperatures ($T_{\delta18O}$) were derived from $\delta^{18}O_{shell}$ values using the $\delta^{18}O_{sw}$ datasets and Eqs. (1) and (2). Regarding the $\delta^{18}O_{sw}$ values used, two different datasets were employed: 1) $\delta^{18}O_{sw}$ used for reconstructing $T_{\delta18O}$ from ventral margin $\delta^{18}O_{shell}$ values for the 55 individuals was that measured during each collection event, and 2) the $\delta^{18}O_{sw}$ value used for temperature reconstruction using $\delta^{18}O_{shell}$ value from the four shells sampled sequentially was the average value measured or interpolated during the days assigned to each $\delta^{18}O_{shell}$ value through the temporal alignment of each carbonate sample.

3.5 Incremental shell growth

In order to determine *P. depressa* shell growth patterns, a sclerochronological study was undertaken. A study of the growth lines/increments allowed us to temporally align each $\delta^{18}O_{shell}$ sample with the calendar dates when the carbonate was deposited. To achieve this objective, first, the thick-section not sampled for isotope analyses was immersed in Mutvei solution for 20 min at 37–40 ºC in order to increase the visibility of the growth lines and increments (Schöne et al., 2005a) (Fig. 2d). Secondly, the thick-sections were studied with sectoral dark-field illumination under a Leica S8APO stereoscopic microscope (8-50x magnification) and with reflected light under a Leica DM 2500M optical microscope (50-100x magnification) at the IIIPC – University of Cantabria (Spain) coupled, in both cases, to a Leica MC190HD digital camera (10MP). Finally, temporal alignment of the stable oxygen isotope record was performed independently of the $\delta^{18}O_{sw}$ sequence following the methods previously applied in other studies (García-Escárzaga et al., 2019; Gutiérrez-Zugasti et al., 2017; Schöne et al., 2007).

Each $\delta^{18}O_{shell}$ data point was aligned with a given number of calendar days based on its position from the shell edge and the counting of the intervening identified major and minor growth lines and increments. Minor growth lines were used to identify fortnightly, daily, and subdaily carbonate accretion units, as well as fortnightly increments. $\delta^{18}O_{shell}$ values were temporally aligned to a variable number of days starting from the shell edge, taking into account the shell collection date and the position of each sample in relation to daily and fortnightly lines. Major growth lines were used for the calendar alignment of growth stoppages. As major growth lines represent growth cessations that are not directly linked to daily or fortnightly tidal rhythms, to properly calibrate the subsequent isotopic samples in time, the first sample after a major growth line was anchored to corresponding predicted $\delta^{18}O_{shell}$ derived from ST and $\delta^{18}O_{sw}$. The independent schlerochronological calendar alignments of $\delta^{18}O_{shell}$ values were then compared to predicted $\delta^{18}O_{shell}$ values based on T_{meas} and $\delta^{18}O_{sw}$ to determine the accuracy of this process and the degree of correlation between $\delta^{18}O_{shell}$ and seawater temperatures for the four sequentially sampled shells. The correlations between measured and predicted $\delta^{18}O_{shell}$ and between $T_{\delta 18O}$ and T_{meas} were calculated on the basis of the coefficient of determination (R^2) derived from a linear regression analysis in Microsoft Excel using the 'Data Analysis' application and regression option.

4. Results

4.1 Shell stable oxygen isotope analyses

The $\delta^{18}O_{shell}$ data obtained from the shell-edges from individuals collected during the same collection event show remarkable concordance (Fig. 3a), with an average standard deviation of +0.14‰. The shells sampled during different parts of the year also show clear seasonal variability in their $\delta^{18}O_{shell}$ values, with higher values (maximum $\delta^{18}O_{shell}$ = +3.17‰) during the colder months and lower values (minimum $\delta^{18}O_{shell}$ = +0.90‰) during the warmer months. A comparison between average $\delta^{18}O_{shell}$ values and predicted $\delta^{18}O_{shell}$ values based on $\delta^{18}O_{sw}$ and T_{meas} for each collection event/sampling event, resulted in a very high statistical correlation ($R^2 = 0.95$; $p < 0.0001$) (Fig. 3b). However, an offset between measured $\delta^{18}O_{shell}$ and predicted $\delta^{18}O_{shell}$ was found. Measured $\delta^{18}O_{shell}$ values were higher by, on average, 1.08 ± 0.15‰ than predicted $\delta^{18}O_{shell}$ values. This offset was found to be stable throughout all seasons (Fig. 3b). Overall, these data suggest that the shells grew in consistent predictable disequilibrium with the ambient seawater.

The results from the four shells sampled sequentially demonstrated marked variability in $\delta^{18}O_{shell}$ values along the growth axis, showing well-defined temporal patterns (Fig. 4) which covered a variable number of cold and warm periods, represented by higher and lower values, respectively. While LAN541, LAN554 and LAN559 exhibited isotopic fluctuations corresponding to approximately one year, LAN545 covered a time span longer than two years. A positive relationship between shell length (Supplementary Material Table 1) and time covered by the $\delta^{18}O_{shell}$ series was observed ($R^2 = 0.80$; $p < 0.0001$). The larger specimen (LAN545) showed stable oxygen isotope variations during 2.5 annual cycles, and the smallest shell (LAN559) covered one year. The maximum and minimum $\delta^{18}O_{shell}$ values (LAN541: +2.76‰, +0.38‰; LAN545: +2.71‰, +0.50‰; LAN554: +2.43‰, +0.59%; LAN559: +2.88‰, +0.50‰) were consistent between the four specimens analysed. On the other hand, slight differences were observed with respect to the trend of the series during the months prior to the collection event. Three of the four shells analysed (LAN541, LAN545 and LAN559) showed collection during a period of decreasing temperatures, just after the annual maximum temperature was reached. Meanwhile, LAN554 demonstrated an increase of the last $\delta^{18}O_{shell}$ value in comparison with the previous one, though with sampling seemingly occurring prior to the annual maximum ST being reached.

4.2 Growth lines/increments

The sclerochronological study carried out on the four Mutvei-stained limpet sections yielded growth rates of different amplitude and periodicity based on analysis of major (annual) and minor (fortnightly, circalunidian and circatidal) growth lines and increments (Fig. 2e; Supplementary Material Fig. 1). Major growth lines were related to a long period of shell growth cessation (from weeks to months). Growth cessation is normally characterised by a change in the orientation of the micro-growth lines/increments and occasionally by high growth rates when the shell resumes its growth. Two types of minor growth lines/increments were recognised: a) subdaily and daily micro-growth lines/increments, and b) fortnightly micro-growth lines. According to the results obtained, a series composed of one micro-growth line and one micro-growth increment represents a tidal cycle (i.e., a circatidal increment) and every bundle composed of two micro-growth lines and two micro-growth increments represents a lunar day (i.e., a circalunidian increment) (Fig. 5c). After 14–15 of these bundles, a prominent growth line is observed, coincident with tidal and lunar cycles (fortnightly increments) (Fig. 5b). These prominent lines and narrower increments were formed during neap tides (first and last quarter moon) (Fig. 5a). A specific area of one limpet section is highlighted in Fig. 5. A comparison between daily predicted $\delta^{18}O_{shell}$ and measured $\delta^{18}O_{shell}$ values, temporally aligned on the basis of the schlerochronological results and adjusted by subtracting the observed mean annual offset (+1.08‰), exhibited a very high correlation ($R^2 = 0.84$; $p < 0.0001$) (Fig. 5d). This result confirms that the periodicity of the accretionary units was properly decoded and the calendar alignment of measured $\delta^{18}O_{shell}$ values was correctly performed.

4.3 Temporal alignment of measured $\delta^{18}O_{shell}$ values

Once the periodicity of the different accretionary units was properly determined, each measured $\delta^{18}O_{shell}$ value was temporally aligned according to subdaily, daily, and fortnightly lines/increments observed from the Mutvei-stained cross sections. To properly compare between measured and predicted $\delta^{18}O_{shell}$ values, the mean annual offset (+1.08‰) was subtracted from measured $\delta^{18}O_{shell}$ values. The results (Fig. 6) for all four of the sequentially sampled shells demonstrated a high correlation between measured and predicted $\delta^{18}O_{shell}$ values ($R^2 = 0.88$-0.94; $p < 0.0001$). The temporal alignment enabled us to study the periods of growth cessation/slowdown. The four specimens analysed were growing during ca. 80-90% of the days covered by the isotopic sequences, although this rate varies between individuals (Table 1). While LAN541 grew during 92% of the days, LAN554 grew only during 75% of the days. In any case, all of the specimens demonstrated that this species does not grow uninterrupted all year-round in northern Iberia (Fig. 6). Winter growth stoppages were observed in all samples during a variable timeframe, although in every case a minimum of six weeks of this season were still represented in the isotopic series (from 40 days in LAN554 to 56 in LAN541 and LAN559). In the case of LAN554, the cessation observed during the last two months of winter also extended into the first week of spring. In addition, LAN545 and LAN554 also reported growth cessations, characterised by a major growth line, from 24th August to 16th September and from 20th July to 23rd September, respectively (Fig. 6).

Daily and seasonal growth rates were estimated on the basis of the measured width of the carbonate sampling paths and the number of days assigned to each $\delta^{18}O_{shell}$ value during the schlerochronologically-based temporal alignment. Results showed that mainly autumn, but occasionally also spring, were the seasons with the highest growth rates (Table 2 and Supplementary Material Fig. 2). Summer was also a period of rapid calcium carbonate deposition rates. By contrast, winter was found to be the season with the lowest growth rates in all shells. Finally, temporal alignment of $\delta^{18}O_{shell}$ values demonstrated that our sequential sampling procedure produced sub-monthly resolution (mean number of days per isotope sample = ca. 5), varying between 2 and 17 days depending on the growth rates. A higher temporal resolution was found in the younger portions of the shell, where growth rates were higher (Table 2 and Supplementary Material Fig. 2).

5. Discussion

5.1 Isotopic equilibrium

The very high statistical correlations observed between measured and predicted $\delta^{18}O_{shell}$ values, in both shell-edge (Fig. 3b) and sequential (Fig. 6) samples, indicates that the *P. depressa* mollusc species precipitates its shell carbonate in consistent disequilibrium with the surrounding ambient seawater. This is in agreement with previous results obtained for other species of *Patella* along the Atlantic coast of Europe (Fenger et al., 2007; Gutiérrez-Zugasti et al., 2017, Ferguson et al., 2011). In our case, a significant offset between measured and predicted $\delta^{18}O_{shell}$ values was found (+1.08‰) for *P. depressa*. A similar positive offset has previously been reported for other *Patella* species. Fenger et al. (2007) and Gutiérrez-Zugasti et al. (2017) published offsets of +0.72‰ and +0.36‰ in *P. vulgata*, respectively. An offset greater than +0.70‰ has also been reported for *Patella caeruela* and *Patella rustica* from different Mediterranean locations (Ferguson et al., 2011; Prendergast and Schöne, 2017). Parker et al. (2017) also reported an offset of +1.30‰ for *Patella candei*, which is higher than that derived from *P. depressa* in this study.

On the basis of published work, an offset from values expected at isotopic equilibrium could be explained by biochemical or metabolic processes generally referred to as "vital effects" (Fenger et al., 2007; Lowenstam and Epstein, 1954, Parker et al., 2017; Wefer and Berger, 1991). Shell biomineralization occurs within the extrapallial space (EPS), an enclosed compartment located between the mantle and the shell. Oxygen and carbon precipitate through CO_2 diffusion across the mantle cavity or through HCO_3^- and CO_3^{2-} undergoing active transport across the epithelium of the mantle (Fenger et al., 2007; Parker et al., 2017; Wheeler, 1992). Different kinetic and metabolic processes, which impact these ion sources, have been invoked to explain carbonate precipitation in disequilibrium. Some studies have noted lower $\delta^{18}O$ in shell carbonate relative to the environment, arguing that kinetic effects lead to lighter isotopes precipitating preferentially (Erez, 1978; McConnaughey, 1989). However, our results, as well as those documented in other limpet studies noted above (Fenger et al., 2007; Parker et al., 2017), show higher $\delta^{18}O$ values than expected under equilibrium conditions. This disequilibrium phenomenon has been explained by the utilization of respired CO_2 during precipitation (Swart, 1983), pH changes in seawater (McConnaughey, 1989), biomineralisation of the shell during evaporative conditions (Schifano and Censi, 1983), and the transport of the lighter isotope out of the shell during biomineralization (Land et al., 1977). Although the exact mechanism remains unknown, the ^{18}O enrichment documented here is an increasingly-documented phenomenon among isotopic limpet studies (Fenger et al., 2007; Parker et al., 2017) and is not, when shown to be consistent, thought to influence the utility of this methodology as a temperature proxy. Significantly, the offset we have discerned for *P. depressa* is consistent and predictable all year-round. As a result, following well-published methodologies (Gutiérrez-Zugasti et al., 2017; Milano et al., 2019), this offset can simply be subtracted from $\delta^{18}O_{shell}$ values obtained to estimate $T_{\delta18O}$.

5.2 *Patella depressa* growth patterns

The sclerochronological analysis, by combining the analysis of shell growth patterns and sequential stable oxygen isotope measurements, has enabled us to decipher the periodicity of the different large- and small-scale accretionary units of the *P. depressa* samples collected. Major growth lines (Fig. 2e) coincided with more extensive growth slowdowns/stoppages in summer and winter. In contrast, minor growth lines/increments exhibited a circatidal periodicity, involving the formation of a microgrowth increment during mollusc submersion and a microgrowth line when molluscs re-emerged. Moreover, fortnightly growth patterns caused by neap and spring tides were also observed. Areas with prominent growth lines and narrower growth increments, followed by areas with narrower growth lines and prominent growth increments, were observed. This tide-controlled shell growth is typically observed in intertidal and subtidal species (Colonese et al., 2017; Milano et al., 2017; Mirzaei et al., 2014; Schöne, 2008), including topshell and limpet taxa previously studied in northern Iberia (García-Escárzaga et al., 2019b; Gutiérrez-Zugasti et al., 2017).

Temporal alignment of the stable isotope data, based on the application of these growth pattern principles, showed that shells grew during ca. 80% of the days during the course of their life span (Table 3), a figure that is higher than that previously obtained for *P. vulgata* in the same coastal area (Gutiérrez-Zugasti et al., 2017). This is likely a product of the varying thermal tolerances of each taxon. While *P. vulgata* is better adapted to cold climate conditions (Poppe and Gotto, 1991), and northern Iberia is close to the southern limit of its latitudinal distribution (Surge et al., 2013), *P. depressa* is a warm-adapted species for which the Cantabrian region represents the approximate centre of its geographical distribution (Fretter and Graham, 1976). This situation means that environmental conditions on the Cantabrian coast are more favourable for *P. depressa* than *P. vulgata*, enabling longer periods of growth throughout the year. Nevertheless, even though climate conditions in northern Iberia are relatively favourable for *P. depressa*, our sclerochronological data show the occurrence of recurrent shell growth cessations in winter, and occasionally also in summer. Molluscs can slow down or even stop precipitation of calcium carbonate throughout their life span as a consequence of environmental and/or physiological reasons, such as thermal extremes, the reproduction cycle, or so-called vital effects (Goodwin et al., 2001; Lazareth et al., 2006; Mannino et al., 2008; Schöne, 2008; Schöne et al., 2002, 2003). For our *P. depressa* samples, winter stoppages occurred during the coldest months of the year, coinciding with the first spawning event of this species (Fernández et al., 2016). However, this part of the reproduction process is unlikely to have influenced the shell growth rate as it aligns with a period of gonadal spreading which, unlike gametogenesis, is not significantly energy demanding (Mannino et al., 2008; Schöne et al., 2005b). In addition, no growth cessation has been observed from April to June when the second spawning event normally occurs (Fernández et al., 2016). Gonadal development did not seemingly influence growth stoppages observed in some specimens during winter, since this biological stage occurs almost all year-round with the exception of summer. Furthermore, variations in salinity or $\delta^{18}O_{sw}$ do not seem to show any significant changes during winter that would allow us to argue that growth rates were driven by one of these environmental variables (Gutiérrez-Zugasti et al., 2015, 2017).

As a result, the growth stoppages observed in this warm-adapted mollusc species during winter are most likely caused by external temperatures dropping below the lower optimal thermal tolerance of the individual, a situation in which the molluscs use most of their available energy to survive (Schöne, 2008). A very similar temperature-driven growth pattern has been previously published for the topshell *P. lineatus* and the limpet *P. vulgata* along the Atlantic façade of Europe (García-Escárzaga et al., 2019b; Gutiérrez-Zugasti et al., 2017; Surge et al., 2013), but also for different mollusc species in other littoral areas across the world (Colonese et al., 2009; Jones and Quitmyer, 1996; Schöne, 2013). Our sclerochronological study also showed that LAN545 and LAN554 stopped their precipitation of calcium carbonate for three and nine weeks in summer, respectively. As no sexual processes (gonadal development and/or gonadal spreading) occur during the warmest months in this species (Fernández et al., 2016) and no significance changes in salinity or $\delta^{18}O_{sw}$ have been observed at the location where shells inhabited (Gutiérrez-Zugasti et al., 2015, 2017), these growth stoppages are potentially initiated by the surpassing of the upper thermal tolerance of some individuals of this species. A similar growth cessation as a consequence of thermal stress during the summer months has also been documented for other warm-adapted species such as *P. lineatus* in the Cantabrian region (García-Escárzaga et al., 2019b) and *Phorcus turbinatus* in the Mediterranean Sea (Mannino et al., 2008).

Although the four sequentially-sampled specimens showed that limpets stopped their growth during winter, the shells which were collected throughout the year and subjected to single ventral margin sampling demonstrated slightly different trends. A comparison between daily predicted $\delta^{18}O_{shell}$ and ventral margin $\delta^{18}O_{shell}$ values, after subtracting the mean annual offset, showed that 8 out of the 10 shells collected during the coldest months correctly cover the maximum predicted $\delta^{18}O_{shell}$ values (Fig. 7), suggesting that these shells did not stop their growth in winter. However, two shells collected in February 2012 (ID codes: LAN424 and LAN426) did not reflect the coldest temperatures observed implying a winter growth cessation. This was also observed for the summer season, when two of the individuals sampled sequentially stopped shell formation. This specimen-specific variability in shell growth patterns, probably driven by higher thermal sensitivity to colder/warmer temperatures in some individuals, has been commonly reported for biogenetic calcium carbonates in molluscs (Prendergast and Schöne, 2017; Schöne, 2008), including topshells and limpets collected at the same location (García-Escárzaga et al., 2019b; Gutiérrez-Zugasti et al., 2017).

Previously published research has also shown that shell growth patterns are often driven by mollusc ontogeny (Schöne, 2008). A decrease in growth rates and a reduction of the thermal tolerance have been observed in different taxa through life, especially in long-lived specimens (Ivany et al., 2003; Román-González et al., 2017; Schöne, 2013), although it has also been reported in short-lived taxa (Fenger et al., 2007; García-Escárzaga et al., 2019b; Gutiérrez-Zugasti et al., 2017; Schöne et al., 2007). According to Guerra and Gaudencio (1986), *P. depressa* has a longevity of around three years. The isotopic profile of the specimen LAN545 represents 2.5 years of growth and shows a reduction in the growth rate through time, especially during the last year in comparison with the previous ones (Table 2 and Supplementary Material Fig. 2) – in agreement with patterns observed from LAN541 and LAN554. The LAN541 series covers three different summer seasons, with the growth rates being higher during the first summer season (2010), suggesting a growth rate reduction throughout time as a consequence of ontogeny. A similar pattern can be observed in LAN554, since 2011 summer and spring had higher growth rates than these same seasons in 2012. In addition, daily growth rates show a decreasing trend during mollusc life span (Supplementary Material Fig. 2).

On the other hand, however, $\delta^{18}O_{shell}$ values recorded during the winter of 2009-2010 in LAN545 are between +0.1 and +0.25‰ higher than those values observed during the subsequent years (Fig. 6b). Taking into account the analytical error of the highest $\delta^{18}O_{shell}$ value per year (< 0.05‰), a difference of 0.1‰ is statistically significant (t-student p-value < 0.05). The lowest $T_{\delta18O}$ (12.5 ºC) derived from this mollusc were observed during winter 2010 since subsequent years did not report $T_{\delta18O}$ lower than 13 ºC, which could suggest that winter growth cessation did not occur during the early stages of mollusc growth but did in later periods. However, the other three shells exhibited lower maximum $\delta^{18}O_{shell}$ values than those observed during the first year of growth in LAN545, suggesting that a lower thermal tolerance during winter is not exclusively driven by ontogeny. Likewise, LAN554 also stopped its growth in the summer of 2012, even though this shell was at an early stage of its life at this point. Therefore, our results show a general ontogenetic trend towards growth cessation/slowdown alongside intra-specific variability in growth patterns.

5.3 Seawater temperature reconstruction ($T_{\delta18O}$)

In order to accurately reconstruct seawater temperatures ($T_{\delta18O}$), the mean annual offset (+1.08‰) was subtracted from measured $\delta^{18}O_{shell}$ values before applying Eq. 1 and 2. $T_{\delta18O}$ obtained from the shell-edge samples of 55 individuals collected throughout the year directly followed the measured instrumental temperature (T_{meas}) variations (Fig. 8), resulting in a significant, high correlation between $T_{\delta18O}$ and T_{meas} ($R^2 = 0.97$; $p < 0.0001$). $T_{\delta18O}$ ranged from 10.6 to 21.0 °C (annual range = 10.4 °C), covering the entire annual range of T_{meas} during collection events (max = 21.0 ºC; min = 11.8 ºC). This comparison between $T_{\delta18O}$ and T_{meas} also showed maximum positive and negative differences of +0.8 and –0.9°C, respectively (Table 3). Results derived from calculated $T_{\delta18O}$ from the four shells sampled sequentially using the determined daily $\delta^{18}O_{sw}$ accurately reproduced variations in T_{meas} throughout the year ($R^2 = 0.88–0.94$; $p < 0.0001$) (Fig. 9). In spite of growth stoppages observed in some annual cycles, maximum and minimum $T_{\delta18O}$ cover the annual range of T_{meas} well (Table 4a). Maximum (summer) temperatures were reconstructed with a mean error of 0.9 ± 1.4 °C, while minimum (winter) temperatures were calculated with an average error of 1.3 ± 0.6 °C (Table 4a). However, these results are biased by significant summer and winter growth stoppages in specimen LAN554 (Fig. 9). When all the individuals are considered together, maximum and minimum annual temperatures can be reconstructed with a minimum error of just –0.4 and +0.5 ºC, respectively (Table 4a).

When calculations were performed using the annual $\delta^{18}O_{sw}$ measurements, instead of the daily $\delta^{18}O_{sw}$ determinations, seawater temperatures were reconstructed with a mean error of –0.8 ± 0.4 and +1.4 ± 0.7 ºC in relation to maximum and minimum T_{meas}, respectively, although the maximum and minimum annual temperatures could be reconstructed with an accuracy of –0.2 and +0.7 ºC if the total range derived from the four shells analysed is considered (Table 4b). When the mean analytical precision of the IRMS (±0.07‰, equivalent to ±0.3 ºC) is also considered, our results suggest that past seawater temperatures can be reconstructed with a mean uncertainty of –1.1 and +1.7 ºC for maximum and minimum temperatures, respectively. Therefore, despite the occurrence of periods of growth cessation, when several annual cycles are available on each shell and several shells are analysed, summer and winter seawater temperatures and annual ranges can be accurately reconstructed using $\delta^{18}O_{shell}$ values of *P. depressa* in northern Iberia. In addition, the use of daily or annual $\delta^{18}O_{sw}$ does not produce significant differences in the $T_{\delta18O}$, suggesting that seawater temperatures can be accurately reconstructed from this new proxy, even where information about seasonal $\delta^{18}O_{sw}$ variations is unavailable.

5.4 Implications for future palaeoclimate and archaeological studies

Reconstructing human-relevant climate change in the past, particularly on seasonal scales, is crucial for understanding the impact of changes in marine and terrestrial environments on human behaviour (Burke et al., 2018; Roberts et al., 2018; Roffet-Salque et al., 2018), as well as to provide better projections of future climate change. For example, characterising the effect of 8.2 cal kyr B.P. cold climate event, caused by a depletion of the thermohaline circulation in the North Atlantic on the Early Holocene (Allen et al., 2007; Thomas et al., 2007), has the potential to help us understand how the current slowdown of the Gulf Stream may impact western European marine environments in the future (Caesar et al., 2018; Dong et al., 2019). However, finding an accurate palaeoclimate proxy with a high enough temporal resolution is not always straightforward. Our modern calibration of *P.*

depressa as a seawater temperature archive has shown that this species can be used to accurately reconstruct environmental conditions throughout periods of shell growth when the daily or mean annual $\delta^{18}O_{sw}$ variations are known (Table 4).

The reconstruction of past seawater temperatures can be restricted because of our limited knowledge of $\delta^{18}O_{sw}$ variation during the past. Despite this difficulty, some methods have been successfully used to overcome this limitation. Hallmann et al. (2013) observed long-term temperature changes from variations in the stable oxygen isotopic composition of marine shells without using any $\delta^{18}O_{sw}$ values to estimate past seawater temperature. Wang et al. (2012) used the current $\delta^{18}O_{sw}$ for seawater temperature reconstruction during the Roman period assuming similar oceanographic conditions over the last 2000 years. Other studies, focused on the last millennium, have reconstructed $\delta^{18}O_{sw}$ from available salinity datasets (Schöne et al., 2004; Wanamaker et al., 2008). For older periods, such as the Mesolithic (9-7.5 cal kyr B.P.), a correction of +0.011‰ in the current $\delta^{18}O_{sw}$ per metre of sea level change (Fairbanks, 1989), coupled to a correction of –0.2‰ or –0.4‰ during the 8.2 cal kyr B.P. according to $\delta^{18}O_{sw}$ depletion in North Atlantic Ocean proposed by Hoffman et al. (2012) and LeGrande et al. (2006), have been used (García-Escárzaga, 2020). For the Upper Palaeolithic, Ferguson et al. (2011) reconstructed seawater temperatures by deconvoluting $\delta^{18}O_{sw}$ from Mg/Ca ratios, although this method has been subject to critique (Graniero et al., 2016; Cobo et al., 2017; García-Escárzaga et al., 2018). Past seawater temperatures can be successfully reconstructed using these methods, although it must be noted that some degree of uncertainty will always be present.

Beyond palaeoclimate conditions, determining the season when archaeological molluscs were collected also has very important implications for better understanding past human subsistence strategies, as well as providing valuable information on season of site occupation and patterns of mobility/sedentism. Although all four sequentially-sampled shells reported growth cessations for several weeks in winter, if these shells had been hypothetically collected in winter then this could still have been deduced from the stable isotopic data. These growth cessations do not cover the whole of the winter (Table 1) and colder seawater temperatures during the recorded winter period are correctly indicated in the isotope profiles (Fig. 9). In addition, if the quartiles system methodology, which is based on the position of the last $\delta^{18}O_{shell}$ value of each shell in relation to the intra-annual $\delta^{18}O_{shell}$ range for each chronology, as well as the trend of the last few sequential $\delta^{18}O_{shell}$ values (Mannino et al., 2003, 2007; Colonese et al., 2009), is used, the maximum $\delta^{18}O_{shell}$ values of every shell would be correctly assigned to the winter season. This result confirms that it would be possible to identify the season of collection of archaeological specimens of this mollusc taxa based on their $\delta^{18}O_{shell}$ values. Stable oxygen isotope series obtained from LAN541, LAN545, and LAN559 showed a collection during a cooling period following the reaching of the annual maximum temperature in the summer of

2012 (Fig. 4), indicating that these shells died at the end of summer or at the beginning of autumn, in agreement with the real collection date on 1st October (Table 1).

By contrast, LAN554 exhibited decreasing $\delta^{18}O_{shell}$ values close to the shell-edge, suggesting a collection during a warming period. According to reconstructed $T_{\delta 18O}$, the last two calcium carbonate samples measured could have been deposited during the third week of July, more than two months before its real collection date. However, a study of the growth patterns on the Mutvei-stained cross section of this limpet revealed a growth line close to the shell edge, demonstrating a significant growth stoppage prior to the deposition of the most recent calcium carbonate samples measured for this limpet. Combining growth line analyses with the isotopic datasets enables accurate temporal alignment at the end of summer or at the beginning of autumn. In summary, our results highlight that season of collection for *P. depressa* can be accurately determined using multi-proxy sclerochronological investigations, combining stable oxygen isotope analyses and incremental shell growth patterns. Based on our research, we would suggest that this taxon represents a potentially significant palaeoclimatic and season of collection proxy at the large number of Holocene archaeological sites where ancient shells of this species are found in high frequency across western Europe. Thus, this species adds to *P. vulgata* (Fenger et al., 2007; Gutiérrez-Zugasti et al., 2017; Surge et al., 2013) and *P. lineatus* (Gutiérrez-Zugasti et al., 2015; García-Escárzaga et al., 2019a; Mannino et al., 2003), as a valuable taxon for biochemically and schlerochronologically reconstructing seasonal resource use and marine environments of the last human foragers along the Atlantic coast of Europe.

6. Conclusions

This first, modern calibration of *P. depressa* as a palaeoclimatic proxy has shown that it deposits its calcium carbonate in predictable isotopic disequilibrium with the surrounding marine environment. A mean annual offset of +1.08‰ has been observed but this is consistent year-round, making it predictable and allowing it to be subtracted from $\delta^{18}O_{shell}$ values before reconstructing seawater temperatures. Reconstructed temperatures using mean annual $\delta^{18}O_{sw}$ correctly reproduced measured maximum and minimum annual seawater temperatures with a maximum uncertainty of ±1 ºC. Our results demonstrate the major potential of this new environmental archive for furture palaeoclimate investigation in northern Iberia, but also more widely along the Atlantic coast of Europe, where this taxon is very abundant in Mesolithic archaeological sites from the Early Holocene. Nevertheless, before conducting oxygen isotope analyses on subfossil shells collected from locations with ST ranges significantly different to that observed in northern Iberia, further sclerochronological studies of modern specimens in these new littoral conditions should be carried out. This is especially the case since latitudinal changes in the growth patterns of limpet shells have been commonly observed (Schöne, 2008), including amongst *P. vulgata* along Atlantic coast of Europe (Surge et al., 2013). From an archaeological perspective, we have shown that stable oxygen isotope analyses of *P. depressa* can be potentially reliably used to reconstruct the season when shells were collected by past human foragers. This information is crucial to understanding the subsistence strategies of the human groups that inhabited littoral areas of Europe in prehistoric times and, more specifically, during the Mesolithic when molluscs were consumed in great numbers by the last hunter-fisher-gatherers and when climate changes may have influenced regional marine and terrestrial environmental conditions and resource availability.

Acknowledgements

This research was performed as part of the projects HAR2016-75605-R and HAR2017-86262-P, funded by the Spanish Ministry of Economy and Competitiveness (MINECO). AGE is currently supported by the Basque Country Postdoctoral Programme (POS_2019_2_0005). This study has also been supported by the Prehistoric Research Consolidated Group of the Basque Country University (IT1223-19), funded by the Basque Country Government. We thank the Fishing Activity Service of the Cantabrian Government for the authorization to collect modern specimens, the Aquaculture Facility of Santander´s Oceanographic Centre for providing the information related to sea surface temperatures and José Ramón Mira Soto for his help measuring salinity. PR and JZ thank the Max Planck Society for Funding. We would also like to thank to Max Plank Institute for Science of Human History (MPI-SHH), Basque Country University (UPV/EHU), Universidad de Cantabria (UC), and Instituto Internacional de Investigaciones Prehistóricas de Cantabria (IIIPC) for providing support. We would also like to thank Roberto Suárez-Revilla, Sara Marzo, Bianca Fiedler, Mary Lucas, Elsa Perruchini and Lucia Agudo-Pérez for their help.

Declaration of interests

The authors declare that they have no known competing financial interests or personal relationships that could have appeared to influence the work reported in this paper.

Supplementary data

Supplementary material

References

Abell, P.I., Hoelzmann, P., 2000. Holocene palaeoclimates in northwestern Sudan: stable isotope studies on molluscs. Global and Planetary Change 26, 1-12.

Allen, J.R., Long, A.J., Ottley, C.J., Pearson, D.G., Huntley, B., 2007. Holocene climate variability in northernmost Europe. Quaternary Science Reviews 26, 1432-1453.

Andrus, C.F.T., 2011. Shell midden sclerochronology. Quaternary Science Reviews 30, 2892-2905.

Bailey, G.N., Deith, M.R., Shackleton, N.J., 1983. Oxygen Isotope Analysis and Seasonality Determinations: Limits and Potential of a New Technique. American Antiquity 48, 390-398.

Baldini, J.U.L., McDermott, F., Hoffmann, D.L., Richards, D.A., Clipson, N., 2008. Very high-frequency and seasonal cave atmosphere PCO2 variability: Implications for stalagmite growth and oxygen isotope-based paleoclimate records. Earth and Planetary Science Letters 272, 118-129.

Bello-Alonso, P., Ozkorta-Escribano, L., Gutiérrez-Zugasti, I., 2015. Un acercamiento al aprovechamiento de los recursos litorales durante el Mesolítico: los invertebrados marinos del abrigo de El Toral III (Llanes, Asturias), in: Gutiérrez Zugasti, I., Cuenca Solana, D., González Morales, M.R. (Eds.), La Investigación Arqueomalacológica en la Península Ibérica: Nuevas Aportaciones. Nadir Ediciones, Santander, pp. 91-99.

Branscombe, T.L., Bosch, M.D., Miracle, P.T., 2020. Seasonal Shellfishing across the East Adriatic Mesolithic-Neolithic Transition: Oxygen Isotope Analysis of Phorcus turbinatus from Vela Spila (Croatia). Environmental Archaeology, 1-14.

Burchell, M., Stopp, M.P., Cannon, A., Hallmann, N., Schöne, B.R., 2018. Determining seasonality of mussel collection from an early historic Inuit site, Labrador, Canada: Comparing thin-sections with high-resolution stable oxygen isotope analysis. Journal of Archaeological Science: Reports 21, 1215-1224.

Burke, A., Riel-Salvatore, J., Barton, C.M., 2018. Human response to habitat suitability during the Last Glacial Maximum in Western Europe. Journal of Quaternary Science 33, 335-345.

Caesar, L., Rahmstorf, S., Robinson, A., Feulner, G., Saba, V., 2018. Observed fingerprint of a weakening Atlantic Ocean overturning circulation. Nature 556, 191.

Carré, M., Bentaleb, I., Blamart, D., Ogle, N., Cardenas, F., Zevallos, S., Kalin, R.M., Ortlieb, L., Fontugne, M., 2005. Stable isotopes and sclerochronology of the bivalve Mesodesma donacium: Potential application to Peruvian paleoceanographic reconstructions. Palaeogeography, Palaeoclimatology, Palaeoecology 228, 4-25.

Cobo, A., García-Escárzaga, A., Gutiérrez-Zugasti, I., Setien-Marquinez, J., González-Morales, M.R., Higuera, J.M., 2017. Automated measurement of Magnesium/Calcium ratios in gastropod shells using Laser-Induced Breakdown Spectroscopy (LIBS) for paleoclimatic applications. Applied Spectrometry 71, 1-9.

Colonese, A.C., Troelstra, S., Ziveri, P., Martini, F., Lo Vetro, D., Tommasini, S., 2009. Mesolithic shellfish exploitation in SW Italy: seasonal evidence from the oxygen isotopic composition of *Osilinus turbinatus* shells. Journal of Archaeological Science 36, 1935-1944.

Colonese, A.C., Verdún-Castelló, E., Álvarez, M., Briz i Godino, I., Zurro, D., Salvatelli, L., 2012. Oxygen isotopic composition of limpet shells from the Beagle Channel: implications for seasonal studies in shell middens of Tierra del Fuego. Journal of Archaeological Science 39, 1738-1748.

Colonese, A.C., Netto, S.A., Francisco, A.S., DeBlasis, P., Villagran, X.S., de Almeida Rocha Ponzoni, R., Hancock, Y., Hausmann, N., Eloy de Farias, D.S., Prendergast, A., Schöne, B.R., da Cruz, F.W., Giannini, P.C.F., 2017. Shell sclerochronology and stable isotopes of the bivalve Anomalocardia flexuosa (Linnaeus, 1767) from southern Brazil: Implications for environmental and archaeological studies. Palaeogeography, Palaeoclimatology, Palaeoecology 484, 7-21.

Coplen, T.B., 1988. Normalization of oxygen and hydrogen isotope data. Chemical Geology: Isotope Geoscience section 72, 293-297.

Crisp, D., 1964. The effects of the severe winter of 1962-63 on marine life in Britain. Journal of Animal Ecology 33, 165-210.

Deith, M., Shackleton, N.J., 1986. Seasonal exploitation of marine molluscs: oxygen isotope analysis of shell from La Riera cave, in: Straus, L.G., Clark, G.A. (Eds.), La Riera cave. Stone age hunter-gatherer adaptations in northern Spain. Arizona State University, Tempe, pp. 199-313.

Dong, S., Baringer, M.O., Goni, G.J., 2019. Slow Down of the Gulf Stream during 1993–2016. Scientific Reports 9, 6672.

Erez, J., 1978. Vital effect on stable-isotope composition seen in foraminifera and coral skeletons. Nature 273, 199-202.

Epstein, S., Lowenstam, H.A., 1953. Temperature-shell-growth relations of recent and interglacial Pleistocene shoal-water biota from Bermuda. The Journal of Geology, 424-438.

Fabre, M., Lécuyer, C., Brugal, J.-P., Amiot, R., Fourel, F., Martineau, F., 2011. Late Pleistocene climatic change in the French Jura (Gigny) recorded in the δ18O of phosphate from ungulate tooth enamel. Quaternary Research 75, 605-613.

Fairbanks, R.G., 1989. A 17.000-year glacio-eustatic sea lever record: influence of glacial melting rates on the Younger Dryas event and deep-ocean circulation. Nature 342, 637-642.

Fenger, T., Surge, D., Schöne, B., Milner, N., 2007. Sclerochronology and geochemical variation in limpet shells (*Patella vulgata*): A new archive to reconstruct coastal sea surface temperature. Geochemistry, Geophysics, Geosystems 8.

Ferguson, J.E., Henderson, G.M., Fa, D.A., Finlayson, J.C., Charnley, N.R., 2011. Increased seasonality in the Western Mediterranean during the last glacial from limpet shell geochemistry. Earth and Planetary Science Letters 308, 325-333.

Fernández, N., Alborés, I., Aceña-Matarranz, S., 2016. Spatial variability of the reproductive cycle and physiological condition of *Patella* spp. (Mollusca Gastropoda) in the NW of the Iberian Peninsula: Implications for exploitation. Fisheries Research 179, 76-85.

Fontanals-Coll, M., Subirà, M.E., Marín-Moratalla, N., Ruiz, J., Gibaja, J.F., 2014. From Sado Valley to Europe: Mesolithic dietary practices through different geographic distributions. Journal of Archaeological Science 50, 539-550.

Fretter, V., Graham, A., 1976. The Prosobranch molluscs of Britain and Denmark. Part 1: Pleurotomariacea, Fissurellacea and Patellacea. Malacological Society of London, London.

Friedman, I., O'Neil, J.R., 1977. Compilation of stable isotope fractionation factors of geochemical interest, in: Fleischer, M. (Ed.), Data of Geochemistry. United States Department of the Interior, Washington, pp. 1-12.

García-Escárzaga, A., 2020. Paleoclima y aprovechamiento de recursos costeros durante el Mesolítico en la región cantábrica (N de Iberia). BAR International Series, 2977. BAR Publishing, Oxford.

García-Escárzaga, A., Clarke, L.J., Gutiérrez-Zugasti, I., González-Morales, M.R., Martínez, M., López-Higuera, J.-M., Cobo, A., 2018. Mg/Ca profiles within archaeological mollusc (*Patella vulgata*) shells: Laser-Induced Breakdown Spectroscopy compared to Inductively Coupled Plasma-Optical Emission Spectrometry. Spectrochimica Acta Part B: Atomic Spectroscopy 148, 8-15.

García-Escárzaga, A., Gutiérrez-Zugasti, I., Cobo, A., Cuenca-Solana, D., Martín-Chivelet, J., Roberts, P., González-Morales, M.R., 2019a. Stable oxygen isotope analysis of *Phorcus lineatus* (da Costa, 1778) as a proxy for foraging seasonality during the Mesolithic in northern Iberia. Archaeological and Anthropological Sciences 11, 5631-5644.

García-Escárzaga, A., Gutiérrez-Zugasti, I., Schöne, B.R., Cobo, A., Martín-Chivelet, J., González-Morales, M.R., 2019b. Growth patterns of the topshell *Phorcus lineatus* (da Costa, 1778) in northern Iberia deduced from shell sclerochronology. Chemical Geology 526, 49-61.

García-Escárzaga, A., Gutiérrez-Zugasti, I., in press. The role of shellfish in the human subsistence during the Mesolithic in Atlantic Europe: an approach from meat yield estimations. Quaternary International. https://doi.org/10.1016/j.quaint.2020.03.003.

Goodwin, D.H., Flessa, K.W., Schöne, B.R., Dettman, D.L., 2001. Cross-Calibration of Daily Growth Increments, Stable Isotope Variation, and Temperature in the Gulf of California Bivalve Mollusk Chione cortezi: Implications for Paleoenvironmental Analysis. PALAIOS 16, 387-398.

Graniero, L., Surge, D., Gillikin, D., Briz i Godino, I.B., Álvarez, M., 2017. Assessing elemental ratios as a paleotemperature proxy in the calcite shells of patelloid limpets. Palaeogeography, Palaeoclimatology, Palaeoecology 465, 376-385.

Grossman, E.L., Ku, T.L., 1986. Oxygen and carbon isotope fractionation in biogenic aragonite: Temperature effects. Chemical Geology: Isotope Geoscience section 59, 59-74.

Guerra, M.T., Gaudencio, M.J., 1986. Aspects of the ecology of Patella spp. on the Portuguese coast. Hydrobiologia 142, 57-69.

Guiry, E.J., Hillier, M., Richards, M.P., 2015. Mesolithic Dietary Heterogeneity on the European Atlantic Coastline: Stable Isotope Insights into Hunter-Gatherer Diet and Subsistence in the Sado Valley, Portugal. Current Anthropology 56, 460-470.

Gutiérrez-Zugasti, I., Andersen, S.H., Araújo, A.C., Dupont, C., Milner, N., Monge-Soares, A.M., 2011. Shell midden research in Atlantic Europe: State of the art, research problems and perspectives for the future. Quaternary International 239, 70-85.

Gutiérrez-Zugasti, I., García-Escárzaga, A., Martín-Chivelet, J., González-Morales, M.R., 2015. Determination of sea surface temperatures using oxygen isotope ratios from *Phorcus lineatus* (Da

Costa, 1778) in northern Spain: Implications for paleoclimate and archaeological studies. The Holocene 25, 1002-1014.

Gutiérrez-Zugasti, I., Suárez-Revilla, R., Clarke, L.J., Schöne, B.R., Bailey, G.N., González-Morales, M.R., 2017. Shell oxygen isotope values and sclerochronology of the limpet Patella vulgata Linnaeus 1758 from northern Iberia: Implications for the reconstruction of past seawater temperatures. Palaeogeography, Palaeoclimatology, Palaeoecology 475, 162-175.

Hallmann, N., Burchell, M., Schöne, B.R., Irvine, G.V., Maxwell, D., 2009. High-resolution sclerochronological analysis of the bivalve mollusk *Saxidomus gigantea* from Alaska and British Columbia: techniques for revealing environmental archives and archaeological seasonality. Journal of Archaeological Science 36, 2353-2364.

Hallmann, N., Burchell, M., Brewster, N., Martindale, A., Schöne, B.R., 2013. Holocene climate and seasonality of shell collection at the Dundas Islands Group, northern British Columbia, Canada—A bivalve sclerochronological approach. Palaeogeography, Palaeoclimatology, Palaeoecology 373, 163-172.

Hausmann, N., Meredith-Williams, M., 2017. Seasonal patterns of coastal exploitation on the Farasan Islands, Saudi Arabia. The Journal of Island and Coastal Archaeology 12, 360-379.

Hawkins, S.J., Moore, P.J., Burrows, M.T., Poloczanska, E., Mieszkowska, N., Herbert, R.J.H., Jenkins, S.R., Thompson, R.C., Genner, M.J., Southward, A.J., 2008. Complex interactions in a rapidly changing world: responses of rocky shore communities to recent climate change. Climate Research 37, 123-133.

Hoffman, J.S., Carlson, A.E., Winsor, K., Klinkhammer, G.P., LeGrande, A.N., Andrews, J.T., Strasser, J.C., 2012. Linking the 8.2 ka event and its freshwater forcing in the Labrador Sea. Geophysical Research Letters 39.

Kendall, M.A., Burrows, M.T., Southward, A.J., Hawkins, S.J., 2004. Predicting the effects of marine climate change on the invertebrate prey of the birds of rocky shores. Ibis 146, 40-47.

Land, L.S., Lang, J.C., Barnes, D.J., 1977. On the stable carbon and oxygen isotopic composition of some shallow water, ahermatypic, scleractinian coral skeletons. Geochimica et Cosmochimica Acta 41, 169-172.

Lazareth, C.E., Putten, E.V., André, L., Dehairs, F., 2003. High-resolution trace element profiles in shells of the mangrove bivalve Isognomon ephippium: a record of environmental spatio-temporal variations? Estuarine, Coastal and Shelf Science 57, 1103-1114.

LeGrande, A., Schmidt, G., Shindell, D., Field, C., Miller, R., Koch, D., Faluvegi, G., Hoffmann, G., 2006. Consistent simulations of multiple proxy responses to an abrupt climate change event. Proceedings of the National Academy of Sciences of the United States of America 103, 837-842.

Leng, M.J., Lewis, J.P., 2016. Oxygen isotopes in Molluscan shell: Applications in environmental archaeology. Environmental Archaeology 21, 295-306.

Lowenstam, H.A., Epstein, S., 1954. Paleotemperatures of the Post-Aptian Cretaceous as Determined by the Oxygen Isotope Method. The Journal of Geology 62, 207-248.

MacClintock, C., 1967. Shell structure of patteloid and bellerophontoid gastropods (Mollusca). Peabody Museum of Natural History, Yale University, Bulletin 22, 1-140.

Mannino, M.A., Spiro, B.F., Thomas, K.D., 2003. Sampling shells for seasonality: oxygen isotope analysis on shell carbonates of the inter-tidal gastropod *Monodonta lineata* (da Costa) from populations across its modern range and from a Mesolithic site in southern Britain. Journal of Archaeological Science 30, 667-679.

Mannino, M.A., Thomas, K.D., Leng, M.J., Piperno, M., Tusa, S., Tagliacozzo, A., 2007. Marine resources in the Mesolithic and Neolithic at the Grotta Dell'Uzzo (Sicily): evidence from isotope analyses of marine shells. Archaeometry 49, 117-133.

Mannino, M.A., Thomas, K.D., Leng, M.J., Sloane, H.J., 2008. Shell growth and oxygen isotopes in the topshell Osilinus turbinatus: resolving past inshore sea surface temperatures. Geo-Mar Lett 28, 309-325.

McConnaughey, T., 1989. ^{13}C and ^{18}O isotopic disequilibrium in biological carbonates: II. *In vitro* simulation of kinetic isotope effects. Geochimica et Cosmochimica Acta 53, 163-171.

Milano, S., Schöne, B.R., Gutiérrez-Zugasti, I., 2020. Oxygen and carbon stable isotopes of Mytilus galloprovincialis Lamarck, 1819 shells as environmental and provenance proxies. The Holocene 30, 65-76.

Milner, N., Craig, O.E., Bailey, G.N., 2007. Shell Middens in Atlantic Europe. Oxbow Books Ltd, Oxford.

Mirzaei, M.R., Yasin, Z., Shau Hwai, A.T., 2014. Periodicity and shell microgrowth pattern formation in intertidal and subtidal areas using shell cross sections of the blood cockle, Anadara granosa. The Egyptian Journal of Aquatic Research 40, 459-468.

Moore, P., Thompson, R.C., Hawkins, S.J., 2007. Effects of grazer identity on the probability of escapes by a canopy-forming macroalga. Journal of Experimental Marine Biology and Ecology 344, 170-180.

Orton, J.H., Southward, A.J., 1961. Studies on the biology of limpets IV. The breeding of *Patella depressa* Pennant on the north Cornish coast. Journal of the Marine Biological Association of the United Kingdom 41, 653-662.

Owen, R., Kennedy, H., Richardson, C., 2002. Experimental investigation into partitioning of stable isotopes between scallop (Pecten maximus) shell calcite and sea water. Palaeogeography, Palaeoclimatology, Palaeoecology 185, 163-174.

Parker, W.G., Yanes, Y., Surge, D., Mesa-Hernández, E., 2017. Calibration of the oxygen isotope ratios of the gastropods *Patella candei crenata* and *Phorcus atratus* as high-resolution paleothermometers from the subtropical eastern Atlantic Ocean. Palaeogeography, Palaeoclimatology, Palaeoecology 487, 251-259.

Pederzani, S., Britton, K., 2019. Oxygen isotopes in bioarchaeology: Principles and applications, challenges and opportunities. Earth-Science Reviews 188, 77-107.

Poppe, G.T., Goto, Y., 1991. European seashells. Vol. I (Polyplacophora, Caudofoveata, Solenogastra, Gastropoda). Verlag Christa Hemmen, Germany.

Prendergast, A.L., Azzopardi, M., O'Connell, T.C., Hunt, C., Barker, G., Stevens, R.E., 2013. Oxygen isotopes from Phorcus (Osilinus) turbinatus shells as a proxy for sea surface temperature in the central Mediterranean: A case study from Malta. Chemical Geology 345, 77-86.

Prendergast, A.L., Stevens, R.E., O'Connell, T.C., Fadlalak, A., Touati, M., al-Mzeine, A., Schöne, B.R., Hunt, C.O., Barker, G., 2016. Changing patterns of eastern Mediterranean shellfish exploitation in the Late Glacial and Early Holocene: Oxygen isotope evidence from gastropod in Epipaleolithic to Neolithic human occupation layers at the Haua Fteah cave, Libya. Quaternary International 407, 80-93.

Prendergast, A.L., Schöne, B.R., 2017. Oxygen isotopes from limpet shells: Implications for palaeothermometry and seasonal shellfish foraging studies in the Mediterranean. Palaeogeography, Palaeoclimatology, Palaeoecology 484, 33-47.

Ribeiro, P.A., Xavier, R., Santos, A.M., Hawkins, S.J., 2009. Reproductive cycles of four species of *Patella* (Mollusca: Gastropoda) on the northern and central Portuguese coast. Journal of the Marine Biological Association of the United Kingdom 89, 1215-1221.

Roberts, P., Stewart, M., Alagaili, A.N., Breeze, P., Candy, I., Drake, N., Groucutt, H.S., Scerri, E.M.L., Lee-Thorp, J., Louys, J., Zalmout, I.S., Al-Mufarreh, Y.S.A., Zech, J., Alsharekh, A.M., al Omari, A., Boivin, N., Petraglia, M., 2018. Fossil herbivore stable isotopes reveal middle Pleistocene hominin palaeoenvironment in ‘Green Arabia’. Nature Ecology & Evolution 2, 1871-1878.

Roffet-Salque, M., Marciniak, A., Valdes, P.J., Pawłowska, K., Pyzel, J., Czerniak, L., Krüger, M., Roberts, C.N., Pitter, S., Evershed, R.P., 2018. Evidence for the impact of the 8.2-kyBP climate event on Near Eastern early farmers. Proceedings of the National Academy of Sciences 115, 8705-8709.

Schifano, G., Censi, P., 1983. Oxygen isotope composition and rate of growth of patella coerulea, monodonta turbinata and M. articulata shells from the western coast of sicily. Palaeogeography, Palaeoclimatology, Palaeoecology 42, 305-311.

Schöne, B.R., 2008. The curse of physiology—challenges and opportunities in the interpretation of geochemical data from mollusk shells. Geo-Mar Lett 28, 269-285.

Schöne, B.R., Lega, J., W. Flessa, K., Goodwin, D.H., Dettman, D.L., 2002. Reconstructing daily temperatures from growth rates of the intertidal bivalve mollusk Chione cortezi (northern Gulf of California, Mexico). Palaeogeography, Palaeoclimatology, Palaeoecology 184, 131-146.

Schöne, B., Tanabe, K., Dettman, D., Sato, S., 2003. Environmental controls on shell growth rates and $\delta^{18}O$ of the shallow-marine bivalve mollusk Phacosoma japonicum in Japan. Marine Biology 142, 473-485.

Schöne, B.R., Freyre Castro, A.D., Fiebig, J., Houk, S.D., Oschmann, W., Kröncke, I., 2004. Sea surface water temperatures over the period 1884–1983 reconstructed from oxygen isotope ratios of a bivalve mollusk shell (Arctica islandica, southern North Sea). Palaeogeography, Palaeoclimatology, Palaeoecology 212, 215-232.

Schöne, B.R., Dunca, E., Fiebig, J., Pfeiffer, M., 2005a. Mutvei's solution: an ideal agent for resolving microgrowth structures of biogenic carbonates. Palaeogeography, Palaeoclimatology, Palaeoecology 228, 149-166.

Schöne, B.R., Houk, S.D., Freyre Castro, A.D., Fiebig, J., Oschmann, W., Kröncke, I., Dreyer, W., Gosselck, F., 2005b. Daily Growth Rates in Shells of Arctica islandica: Assessing Sub-seasonal Environmental Controls on a Long-lived Bivalve Mollusk. PALAIOS 20, 78-92.

Schöne, B.R., Rodland, D.L., Wehrmann, A., Heidel, B., Oschmann, W., Zhang, Z., Fiebig, J., Beck, L., 2007. Combined sclerochronologic and oxygen isotope analysis of gastropod shells (Gibbula cineraria, North Sea): life-history traits and utility as a high-resolution environmental archive for kelp forests. Marine Biology 150, 1237-1252.

Schulting, R.J., Richards, M.P., 2001. Dating Women and Becoming Farmers: New Palaeodietary and AMS Dating Evidence from the Breton Mesolithic Cemeteries of Téviec and Hoëdic. Journal of Anthropological Archaeology 20, 314-344.

Surge, D., Wang, T., Gutierrez-Zugasti, I., Kelley, P.H., 2013. Isotope sclerochronology and season of annual growth line formation in limpet shells (*Patella vulgata*) from cold- and warm-temperate zones in the eastern North Atlantic. PALAIOS 28, 386-393.

Swart, P.K., 1983. Carbon and oxygen isotope fractionation in scleractinian corals: a review. Earth-Science Reviews 19, 51-80.

Thomas, E.R., Wolff, E.W., Mulvaney, R., Steffensen, J.P., Johnsen, S.J., Arrowsmith, C., White, J.W.C., Vaughn, B., Popp, T., 2007. The 8.2ka event from Greenland ice cores. Quaternary Science Reviews 26, 70-81.

Hawkins, S.J., Moore, P.J., Burrows, M.T., Poloczanska, E., Mieszkowska, N., Herbert, R.J.H., Jenkins, S.R., Thompson, R.C., Genner, M.J., Southward, A.J., 2008. Complex interactions in a rapidly changing world: responses of rocky shore communities to recent climate change. Climate Research 37, 123-133.

Wanamaker, A.D., Kreutz, K.J., Borns, H.W., Introne, D.S., Feindel, S., Funder, S., Rawson, P.D., Barber, B.J., 2007. Experimental determination of salinity, temperature, growth, and metabolic effects on shell isotope chemistry of *Mytilus edulis* collected from Maine and Greenland. Paleoceanography 22, PA2217.

Wanamaker, A.D., Kreutz, K.J., Schöne, B.R., Pettigrew, N., Borns, H.W., Introne, D.S., Belknap, D., Maasch, K.A., Feindel, S., 2008. Coupled North Atlantic slope water forcing on Gulf of Maine temperatures over the past millennium. Climate Dynamics 31, 183-194.

Wanamaker, A.D., Hetzinger, S., Halfar, J., 2011. Reconstructing mid- to high-latitude marine climate and ocean variability using bivalves, coralline algae, and marine sediment cores from the Northern Hemisphere. Palaeogeography, Palaeoclimatology, Palaeoecology 302, 1-9.

Wang, T., Surge, D., Mithen, S., 2012. Seasonal temperature variability of the Neoglacial (3300–2500 BP) and Roman Warm Period (2500–1600 BP) reconstructed from oxygen isotope ratios of limpet shells (*Patella vulgata*), Northwest Scotland. Palaeogeography, Palaeoclimatology, Palaeoecology 317–318, 104-113.

Wefer, G., Berger, W.H., 1991. Isotope paleontology: growth and composition of extant calcareous species. Marine Geology 100, 207-248.

Wheeler, A., 1992. Mechanisms of molluscan shell formation. Calcification in biological systems, 179-216.

Figure 1. Location of the study area in northern Spain and Langre Beach.

Figure 2. a) Modern specimen of *Patella depressa*. Dashed lines indicate the cutting axis from which two think sections (b and d) were obtained for sclerochronological analyses. Dashed arrows show methodology applied to take a carbonate sample from the shell edge. b) Cross section of a limpet shell. c) Portion of a cross section showing the calcite layer and the visible growth lines. d) Mutvei´s-stained cross section. e) Portion of a cross section stained with Mutevei´s solution displaying major and minor growth lines.

Figure 3. a) Comparison between measured stable oxygen isotope values ($\delta^{18}O_{shell}$) from shell edge samples (five per collection event) and daily predicted $\delta^{18}O_{shell}$ using instrumental temperatures and $\delta^{18}O_{water}$ and Eqs. (1) and (2). b) Mean $\delta^{18}O_{shell}$ from shell edge samples collected at the same date compared with predicted $\delta^{18}O_{shell}$ using instrumental temperatures and $\delta^{18}O_{water}$ and Eqs. (1) and (2). Error bars were calculated using 1σ SD of the five shells measured per collection event.

Figure 4. Stable oxygen isotope values ($\delta^{18}O_{shell}$) from the four shells sampled sequentially (LAN-541, LAN-545, LAN-554 and LAN-559). Results show a clear sinusoidal pattern related to seasonal variations. DoG: direction of growth.

Figure 5. Sclerochronology and temporal alignment of a growth area of shell LAN545 corresponding to 15 weeks, between 29th March 2012 and 10th July 2012. a) During that time, the shell underwent a total of seven spring tides (open circles: full moon; filled circles: new moon) and eight neap tides (circles open to the left or right: first and last quarter moon, respectively). The maximum and

minimum height reported for the tide cycle was 5.1 m during high tide and 0.6 m during low tide. b) Mutvei´s-stained cross section exhibited a series of microgrowth lines and increments formed with different periodicity. Dashed lines indicate the occurrence of fortnight lines every 14-15 days, coincident with neap tides. DoG: direction of growth. c) Detailed look at growth lines/increments with a circatidal and circalunial periodicity. d) Measured $\delta^{18}O_{shell}$ values were temporally aligned with daily predicted $\delta^{18}O_{shell}$, assigning each $\delta^{18}O_{shell}$ value to a variable number of days according to the number of tidal cycles covered by each sample spot. Therefore, a variable number of daily predicted $\delta^{18}O_{shell}$ values were assigned to each measured $\delta^{18}O_{shell}$ value. In order to obtain a correlation between measured $\delta^{18}O_{shell}$ values and predicted $\delta^{18}O_{shell}$ values, all of the daily predicted $\delta^{18}O_{shell}$ values assigned to each measured $\delta^{18}O_{shell}$ values were considered. Measured $\delta^{18}O_{shell}$ values and predicted $\delta^{18}O_{shell}$ showed high correlation ($R^2 = 0.84$, $p < 0.0001$). Red dashed line showed a theoretical 1:1 line with a slope = 1.

Figure 6. Calendar-aligned shell stable oxygen isotope values ($\delta^{18}O_{shell}$) of shells sampled sequentially: a) LAN541, b) LAN545, c) LAN554 and d) LAN559). The calendar alignment was completed by using fortnightly and daily increments observed in cross-section. All $\delta^{18}O_{shell}$ series showed a high correlation with predicted $\delta^{18}O_{shell}$ from daily T_{meas} and $\delta^{18}O_{water}$. Grey bars show periods of growth cessation determined by sclerochronological analysis, which mainly occurred in winter. All $\delta^{18}O_{shell}$ series showed a high correlation with predicted $\delta^{18}O_{shell}$ from daily T_{meas} and $\delta^{18}O_{water}$.

Figure 7. Comparison between mean $\delta^{18}O_{shell}$ from shell edge samples collected at the same date after subtracting mean annual offset and predicted $\delta^{18}O_{shell}$ using instrumental temperatures and $\delta^{18}O_{water}$ and Eqs. (1) and (2). Error bars were calculated using 1σ SD of the five shells measured per collection event.

Figure 8. Mean $T_{\delta18O}$ from shell ventral margin samples compared with T_{meas}. Error bars were calculated using 1σ SD of the five samples measured by collection event. Results show a sinusoidal pattern related to seasonal variations in temperature and strong correlation between variables.

Figure 9. Calendar-aligned reconstructed temperatures ($T_{\delta18O}$). Time calibration was the same as for the $\delta^{18}O_{shell}$. Grey bars show periods of growth cessation determined by sclerochronological analysis which mainly occurred in winter. Error bars were calculated from $\delta^{18}O_{water}$ variability that occurred during the day(s) in which the sampled shell portion was formed plus the analytical precision of the mass spectrometer for each $\delta^{18}O_{shell}$ value. All $T_{\delta18O}$ series showed a high correlation with instrumental temperatures (T_{meas}).

Table 1. Number of growth stop days per season and number total of days of shell growth for each specimen.

Sample	**2012**			**2011**		**2010**	**Total days growth**	
	Summer	Spring	Winter	Summer	Winter	Summer	n	%
LAN541	0	0	35	0	---	---	428	92.4
LAN545	23	0	48	0	73	25	764	81.9
LAN554	63	11	60	---	---	---	409	75.3
LAN559	0	0	35	---	---	---	343	90.7

Table 2. Average daily increment width (µm) per season.

Seasonal growth rate per day (µm)											
Sample	2012			2011				2010			
	Summer	Spring	Winter	Autumn	Summer	Spring	Winter	Autumn	Summer	Spring	Winter
LAN541	32.4	27.2	8.3	58.9	29.8	---	---	---	---	---	---
LAN545	17.4	11.4	5.4	22.6	16.3	19.5	7.6	18.4	17.2	22.4	---
LAN554	4.2	11.9	3	35.5	28.3	38.1	---	---	---	---	---
LAN559	22.6	41.8	10.7	43.4	---	---	---	---	---	---	---

Table 3. Difference between instrumental temperatures (T_{meas}) and reconstructed temperatures ($T_{\delta 18O}$) from shell edge samples.

Collection date	**Average $T_{\delta 18O}$ (ºC)**	**SD**	**T_{meas} (ºC)**	**Difference $T_{meas} - T_{\delta 18O}$ (ºC)**
12-10-2011	18.0	0.5	17.9	-0.1
25-11-2011	15.7	0.6	16.1	+0.4
12-01-2012	13.7	1.1	13.6	-0.1
10-02-2012	12.7	1.7	11.8	-0.9
11-03-2012	12.4	0.7	12.5	+0.1
22-04-2012	12.3	0.8	13.0	+0.7
03-06-2012	16.1	0.5	15.3	-0.9
22-07-2012	20.0	0.5	19.4	-0.7
05-08-2012	20.2	0.3	21.0	+0.8
10-09-2012	20.0	0.6	20.5	+0.5

01-10-2012	18.3	0.7	19.1	+0.8
Mean	16.3	0.7	16.4	0.5
Max	20.2	1.7	21.0	0.9
Min	12.3	0.3	11.8	0.1
Range	7.8	1.4	9.2	0.8

Table 4. Difference between maxima and minima instrumental temperatures (T_{meas}) and maxima and minima reconstructed temperatures ($T_{\delta 18O}$) from shells sampled sequentially using data on a) daily $\delta^{18}O_{water}$ and b) mean annual $\delta^{18}O_{water}$.

a	**Daily $\delta^{18}O_{water}$**						
	ID Sample	Maximum $T_{\delta 18O}$ (°C)	Maximum T_{meas} (°C)	Difference with Maximum T_{meas} (°C)	Minimum $T_{\delta 18O}$ (°C)	Minimum T_{meas} (°C)	Difference with Minimum T_{meas} (°C)
	LAN541	23.6	23.1	+0.5	12.1	11.1	+1.0
	LAN545	22.7	23.1	-0.4	12.9	11.0	+1.9
	LAN554	19.9	23.1	-3.2	13.0	11.1	+1.9
	LAN559	22.7	23.1	-0.4	11.6	11.1	+0.5
	Mean	22.2	23.1	-0.9	12.4	11.1	+1.3
	SD	1.4	0.0	1.4	0.6	0.0	0.6

b	**Mean annual $\delta^{18}O_{water}$**						
	ID Sample	Maximum $T_{\delta 18O}$ (°C)	Maximum T_{meas} (°C)	Difference with Maximum T_{meas} (°C)	Minimum $T_{\delta 18O}$ (°C)	Minimum T_{meas} (°C)	Difference with Minimum T_{meas} (°C)
	LAN541	22.9	23.1	-0.2	12.0	11.1	+0.9
	LAN545	22.3	23.1	-0.8	12.5	11.0	+1.5
	LAN554	21.9	23.1	-1.2	13.7	11.1	+2.6
	LAN559	22.1	23.1	-1.0	11.8	11.1	+0.7
	Mean	22.3	23.1	-0.8	12.5	11.1	+1.4
	SD	0.4	0.0	0.4	0.7	0.0	0.7

Highlights

- First sclerochronological study conducted on limpet *Patella depressa*
- $\delta^{18}O_{shell}$ data showed that $CaCO_3$ is deposited close to isotopic equilibrium ($R^2 = 0.95$)
- *P. depressa* is a high-resolution palaeothermometer in the Atlantic Europe
- Results have significant implication for future palaeoclimate and archaeological investigation